Engineering Failure Analysis xxx (2009) xxx–xxx

Contents lists available at ScienceDirect

Engineering Failure Analysis

journal homepage: www.elsevier.com/locate/engfailanal

Effect of mechanical mismatching on the ductile-to-brittle transition curve of welded joints

R. Lezcano [a], C. Rodríguez [b], I. Peñuelas [b], C. Betegón [b], F.J. Belzunce [b,*]

[a] Arcelor-Mittal, Veriña, Gijón, Spain
[b] Universidad de Oviedo, E.P.S. de Ingenieria de Gijon, Dpto. ciencia de Materiales, Campus Universitario (Edificio Este), 33203 Gijón (Asturias), Spain

ARTICLE INFO

Article history:
Received 23 February 2009
Accepted 10 April 2009
Available online xxxx

Keywords:
Ductile-to-brittle transition
Constraint parameter
Welded joints

ABSTRACT

The effect of mechanical mismatching (ratio between the yield strength of base and weld metal) on the toughness of welded joints at different temperatures was analysed and the ductile-to-brittle transition curves of these welded joints were experimentally obtained. The filler metal of the joints was always the same, varying the base metal and the width of the welded zone. Two base metals were selected, one with a higher strength than the filler metal (undermatched joint) and the other with a lower strength than the filler metal (overmatched joint). In addition, the joints were made using two different weld widths, 20 and 10 mm.

The fracture behaviour of the joints were determined at different temperatures using SE(B) specimens provided with short cracks ($a/W = 0.22$). Besides, long crack specimens ($a/W = 0.5$) were also used for comparison. In the case of overmatched joints, the J-values for ductile crack growth are larger than for the undermatched joints. In addition, the ductile-to-brittle transition curve is displaced towards lower-temperatures and higher-toughness values and the toughness for cleavage fracture is also larger for overmatching than for undermatching. All these effects are more significant as the weld width decreases and a have been explained in terms of constraint modifications.

1. Introduction

When making welding joints, small discontinuities, voids and other defects cannot be absolutely avoided and the heterogeneity of the own joint along with the presence of residual stresses may be taken into account in order to prevent failures and to assure the integrity of the whole component or structure. One of the key factors for understanding the fracture behaviour of any welded structure containing cracks is the heterogeneity of the joint. In an ideal weld, where a crack is contained within the weld metal and can grow parallel to the weld metal-base metal interface, assuming that the effect of the heat affected zone is negligible [1,2], a two material idealisation of the weld can be used. Fig. 1 shows this idealisation: a weld metal (WM) with a yield strength σ_{0w} and width $2h$ containing the crack and a base metal (BM) with a yield strength σ_{0b}. The level of material mismatching can be defined by the mismatch ratio M, given by:

$$M = \sigma_{0w}/\sigma_{0b} \quad (1)$$

with $M > 1$ referring to an overmatching situation and $M < 1$ to an undermatching one, being $M = 1$ the case of an homogeneous specimen in which the weld metal is identical to the base metal.

* Corresponding author. Tel.: +34 985 18 2024; fax: +34 985 18 20 22.
E-mail address: belzunce@uniovi.es (F.J. Belzunce).

1350-6307/$ - see front matter © 2009 Elsevier Ltd. All rights reserved.
doi:10.1016/j.engfailanal.2009.04.030

Nomenclature

A	crack length
Δa	crack length increment
B	specimen thickness
h	weld semi-width
J	J-integral
J_{mat}	J under high constraint
J^C_{mat}	J at unstable fracture and specified level of constraint
k	exponent in Ainswtorth and O'Dowd's constraint correction
K_I	stress intensity factor in mode I of load
K_{mat}	fracture toughness measured under high constraint
K^C_{mat}	fracture toughness at unstable fracture and specified level of constraint
K_r	fracture ratio
m	shape parameter of the Beremin cleavage fracture model
M	mismatch ratio (level of mismatching)
Q	constraint Q-parameter (triaxiality parameter)
r, θ	polar coordinates with origin at the crack tip
R	R-curve (resistance curve)
SE(B)	single edge notched specimen
T	temperature
T_c	T-stress
W	specimen width
β_g	geometrical constraint parameter (biaxiality parameter)
β_m	constraint parameter due to material mismatching
β_T	total constraint parameter
ξ	parameter in Ainswtorth and O'Dowd's constraint correction
σ	stress
σ_0	yield strength
σ_{0b}	yield strength of the base metal
σ_{0w}	yield strength of the weld metal
τ	normalised T-stress

Using finite element methods and slip-line field theories, Hao et al. [3], Joch et al. [4] and Burstow and Ainsworth [5,6] have demonstrated that material strength mismatching significantly affects both the stress fields and the crack resistance curves obtained with specimens submitted to tension and bending. They found that the magnitude of the stress distribution around the crack tip depends not only on the applied load but also on the level of the mismatch ratio M and the weld width $2h$. In the case of overmatching ($M > 1$), the crack tip stress fields decrease in relation to those obtained in homogeneous material ($M = 1$) and, conversely, the stress fields are raised in the case of undermatching ($M < 1$).

Fracture toughness of welds with a crack growing into the weld metal, which is surrounded by the base metal, is also affected by the weld width, as a result of the size of the plastic zone developed in front of the crack tip, which conditions the stress field [7]. As long as the plastic zone is large enough to attain the base metal, the plastic behaviour of the weld joint modifies. When the base metal is stronger than the weld metal ($M < 1$: undermatching), the plastic field will be lower and the stress level higher, giving way to a larger constraint, and the opposite takes place in the case of overmatching. In a narrow weld, the plastic zone will attain the base metal sooner and the mentioned effect can be observed before.

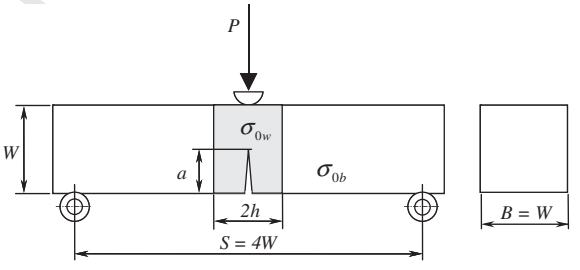

Fig. 1. Two material idealisation of a three-point bend mismatched specimen.

Please cite this article in press as: Lezcano R et al. Effect of mechanical mismatching on the ductile-to-brittle transition curve of welded joints. Eng Fail Anal (2009), doi:10.1016/j.engfailanal.2009.04.030

As a result of these works, constraint has to be considered not only as a function of the geometry but also due to material mismatching [7,8].

Geometrical constraint can be quantified by means of both the elastic *T*-stress [9,10], which directly characterises the geometrical constraint effect and the non-linear *Q*-parameter [11,12], which is a direct measure of the elastic-plastic stress field that can be related with the HRR field [13,14], and it usually describes the deviation of the stress field from the reference stress state at a specified position ahead of the crack tip, thus

$$Q = \frac{\sigma_{\theta\theta} - \sigma_{\theta\theta}^{\mathrm{Ref}}}{\sigma_0} \text{ at } \frac{r\sigma_0}{J} = 2, \quad \theta = 0. \tag{2}$$

where σ_0 is the material yield strength and $\sigma_{\theta\theta}^{\mathrm{Ref}}$ is the stress distribution when $T_c = 0$. On the basis of a dimensional argument, O'Dowd and Shih [11] demonstrated that under small scale yielding, Q and T_c are univocally related for each material by expressions of the form:

$$Q = A\tau + B\tau^2 + C\tau^3 \tag{3}$$

where $\tau = T_c/\sigma_0$ is the normalised T-stress. The evolution of T with the load can be characterised by the so-called biaxiality parameter or geometrical constraint parameter, β_g, so that for each geometry the value of the *T*-stress is defined by an expression of the form:

$$T_c = \frac{\beta_g K_I}{\sqrt{\pi a}} \tag{4}$$

Geometries with positive β_g values lead to positive *T*-stresses and this fact slightly raises the stress fields. Conversely, geometries with negative β_g values lead to negative *T*-stresses and the stress fields significantly decrease.

In order to quantify constraint due to material mismatching, different methodologies based on that used to quantify geometrical constraint have been used. Thawlow and colleagues [15,16] defined a procedure similar to the *J*–*Q* one and Betegón and Peñuelas [7] follow a procedure similar to the J–T_c one. In this latter case, they developed a J–T_g–T_m formulation, where J is related to the applied load, T_g with the geometrical constraint and T_m with the material constraint, and defined a material constraint parameter, β_m, for overmatched welded joints, that quantifies the material mismatching effect on the crack tip stress fields. In the case of specimens like the one show in Fig. 1, both geometry and material mismatching affect the crack tip stress fields and a total constraint parameter β_t ($\beta_t = \beta_g + \beta_m$) can be used to describe the whole constraint. Nevertheless, constraint parameter β_m cannot be defined in undermatching situations.

On the other hand, it is known that the geometry of the specimen significantly affects the crack resistance curve. Fracture resistance is determined by the operative failure micromechanism which depends on temperature. At low temperatures, the operative micromechanism is cleavage. However, at higher temperatures, the operative micromechanism is ductile tearing. In a range of intermediate temperatures, known as the transition zone, fracture is initiated by ductile tearing, but final fracture is produced by a sudden cleavage failure. It has been determined not only numerically but also experimentally, that geometries with low constraint are more resistant to both cleavage fracture and ductile tearing than geometries with high constraint. Thus, the transition curves for the different geometries were obtained by different authors, e.g. in Amar and Pineau [17], Gao et al. [18] and Hausild at al. [19].

The transition curves corresponding to different welded joints have been determined in this paper. To do this, different configurations of welded joints were analysed by means of the finite element method [20] and an experimental program was carried out. In all the analysed mismatch cases, the weld metal is assumed to be the same, and both the base metal and its width were modified in order to attain different constraint conditions.

2. Micro-mechanical models

Cleavage fracture was described by means of the statistical model proposed by Beremin to describe the fracture of ferritic steels [21], in which the local stress is used to determine the fracture probability. This model is based on the Weibull weakest link theory. In addition, the failure probability corresponding to any material point subjected to a certain load history can be understood as the non-survival probability of the point at a certain time, and is determined by the maximum load level attained up to this time, which is obtained by means of the Weibull stress. Thus, the failure probability can be written in the form

$$P_f = 1 - \exp\left[-\left(\frac{\sigma_w}{\sigma_u}\right)^m\right] \tag{5}$$

where σ_u is a scaling stress and σ_w is the Weibull stress, defined by

$$\sigma_w = \left[\frac{1}{V_0} \cdot \int (\sigma_1 - \sigma_{th})^{m_s} dV\right]^{1/m_s} \tag{6}$$

Please cite this article in press as: Lezcano R et al. Effect of mechanical mismatching on the ductile-to-brittle transition curve of welded joints. Eng Fail Anal (2009), doi:10.1016/j.engfailanal.2009.04.030

Thus, the Weibull stress, which determines the fracture probability, depends on the reference volume, V_0, the shape parameter, m, and the maximum applied principal stress σ_1, whilst σ_{th} is the threshold stress that defines the minimum stress value that can produce stable crack growth.

Under these assumptions, the Beremin model has three characteristic parameters: m, σ_u and σ_{th} which have to be fitted using both numerical and experimental results. The shape parameter m is temperature-independent, whilst both σ_u and σ_{th} are temperature-dependent, Wasiluk and co-workers [22].

On the other hand, the micromechanical model considered in this paper for ductile propagation, is the so-called complete Gurson model (Zang et al. [23]), that combines the Gurson–Tvergaard–Needleman model (e.g. [24–28]) and the plastic-limit-load coalescence criterion proposed by Thomason [29,30]. In this complete model, the process of ductile failure, which comprises nucleation, growth and coalescence of microvoids, is described by a modified yield function expressed in the form

$$\Phi(q,p,\bar{\sigma},f) = \left(\frac{q}{\bar{\sigma}}\right)^2 + 2\cdot q_1\cdot f^*\cdot\cosh\left(-\frac{3\cdot q_2\cdot p}{2\cdot\bar{\sigma}}\right) - (1+q_3\cdot f^{*2}) = 0 \tag{7}$$

where q is the macroscopic von Mises effective stress given by the deviatoric components of the Cauchy stress, p is the hydrostatic stress, $\bar{\sigma}$ is the material flow stress (which relates to the equivalent plastic strain by means of an uniaxial equation in the form $\bar{\sigma} = H(\bar{\varepsilon}^p)$), and f is the current void volume fraction. The constants q_1, q_2 and q_3 are fitting parameters which depend on the material, and f^* is the modified void volume fraction (related to f) introduced by Tvergaard and Needleman [28] to predict the rapid loss in strength that accompanies void coalescence. Ductile fracture is described by means of the evolution law for the void volume fraction, f, from an initial porosity value, f_0, to the void volume fraction at final failure, f_F.

Gurson's parameters have been considered temperature-independent. This hypothesis agrees with the physical sense of these microstructural parameters, and with the results of Pardoen and Hutchison [31].

3. Materials and experimental procedure

Specimens extracted from overmatched and undermatched welded joints have been obtained making use of one weld metal (WM) and two base metal (BM1) and (BM2), with short and long cracks and different weld widths and have been tested within a complete experimental program. The lower yield strength base metal (BM1) was an S275JR steel (0.11% C) and the higher yield strength base metal (BM2) was an F-1 steel with 0.18% C. The thickness of the steel sheets used as base metal was 20 mm in order to assure a condition of plane strain.

A welding procedure has been developed in order to obtain welded joints without mechanical and geometrical discontinuities and with a heat affected zone (HAZ) so small to consider a two-material idealisation welded joint (only base and weld metal). An appropriate joint geometry was also required to obtain specimens where the crack is forced to grow within the weld metal. Thus, in the case of welded joints with large widths ($2h$ = 20 mm), a multi-pass open square butt weld deposited from both sides was employed. However, in the case of a narrow width ($2h$ = 10 mm), due to accessibility problems, a multi-pass single V-butt weld using backing strip and full penetration from a single side was selected. The optimal operational and metallurgical conditions have been attained using a semiautomatic mechanically operated welding process with metal active shielding gas (GMAW). The welding parameters are described in Table 1.

Welded coupons were finally inspected using non-destructive tests, which included visual, X-ray and ultrasonic inspections. Fig. 2a shows a macrography of a narrow width overmatched weld and Fig. 2b corresponds to a large width undermatched weld.

Tensile and SE(B) fracture toughness specimens were extracted and machined according to the scheme shown in Fig. 3.

The tensile properties of the weld and base metals have been determined at room temperature and also at low temperature (until −60 °C) according to the ASTM E9 M standard [32], using round 10 mm diameter specimens. The base metal specimens had a calibrated length of 70 mm and were extracted in the longitudinal direction, parallel to the weld direction. The weld metal specimens were extracted in the transverse direction and had a calibrated length of 20 mm.

Single edge bend specimens (SE(B)) with their longitudinal direction perpendicular to the weld direction have been used for estimating the crack growth resistance curves (J–R curves) and the fracture toughness of the welded joints (see Fig. 3). The specimens were notched, fatigue pre-cracked and sidegrooved. The notch was located in the centre line of the weld metal and the crack was grown into the thickness direction until attaining a crack length to specimen width, a/W = 0.22 and 0.5. All the specimens had a width and thickness of 20 mm ($B = W$) and the span length was $4W$. Fig. 1 shows the single edge

Table 1
Welding parameters.

Shielding gas	88% Ar + 12% CO_2
Welding wire	E-70 S6 (1 mm diameter)
Welding current	140–200 A
Welding voltage	20–25 V
Welding speed	20–30 cm/min
Heat input	10 kJ/cm
Interpass temperature	<250 °C

Please cite this article in press as: Lezcano R et al. Effect of mechanical mismatching on the ductile-to-brittle transition curve of welded joints. Eng Fail Anal (2009), doi:10.1016/j.engfailanal.2009.04.030

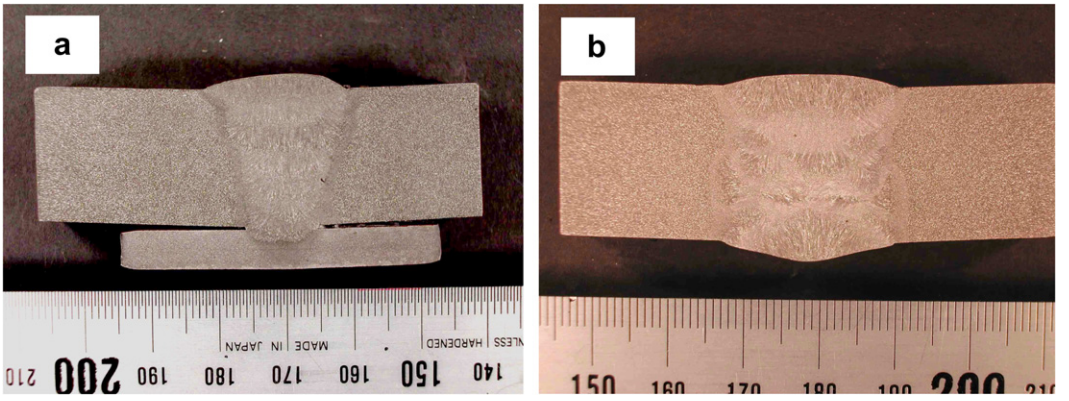

Fig. 2. (a) Macrography of a narrow width overmatched weld ($2h$ = 10 mm) and (b) macrography of a large width undermatched weld ($2h$ = 20 mm).

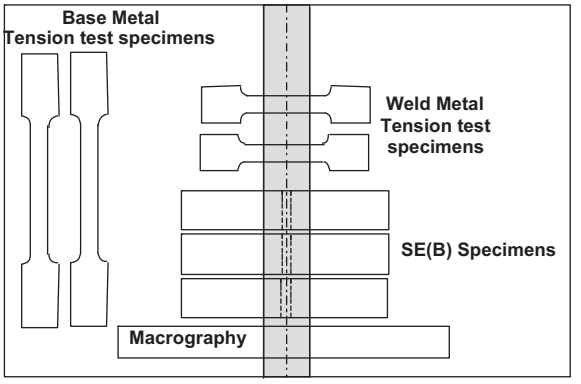

Fig. 3. Specimen extraction from the welded coupons.

Table 2
Specimen configurations and denominations for fracture characterisation.

Denomination	M	a/W	$2h$ (mm)
A	>1	0.22	10
B	>1	0.22	20
C	<1	0.22	10
D	<1	0.22	20
E	<1	0.5	20

bend test specimen geometry and Table 2 the different specimen configurations used in the work and their denominations. All the selected configurations had short cracks except the E one, as it was numerically demonstrated in [33] that in the case of long cracks the fracture behaviour of these configurations are not significantly modified. Two short crack configurations were overmatched (A and B), the two others undermatched (C and D), two of them had narrow weld zones (A and C) and the others large ones (B and D).

Fracture tests were carried out at room and low temperatures (20, 10, 0, −20, −40, −50 and −60 °C) in accordance with the ASTM E1280-05a standard [34] and the single specimen method was used to determine the J–R curves. This method allows to indirectly obtain the growth of the crack during the test by means of the variation of the specimen compliance. However, as this method leads to significant inaccuracies when testing very ductile materials and short crack specimens, a colour marking technique of the crack front has been applied, which allowed us to make two direct physical measurements of the crack during each test: an intermediate crack length was measured by paint spraying the open crack front and the final crack length was also marked after applying a fatigue load before the final breakage of the specimen. Fig. 4 shows the fracture surfaces of one of these specimens where the two aforementioned crack fronts are clearly seen. In a post-analysis of the experimental results, the crack growth values, Δa, indirectly obtained using the compliance method have first been corrected to match the values physically measured on the fracture surface, and then they have been interpolated between these values.

Please cite this article in press as: Lezcano R et al. Effect of mechanical mismatching on the ductile-to-brittle transition curve of welded joints. Eng Fail Anal (2009), doi:10.1016/j.engfailanal.2009.04.030

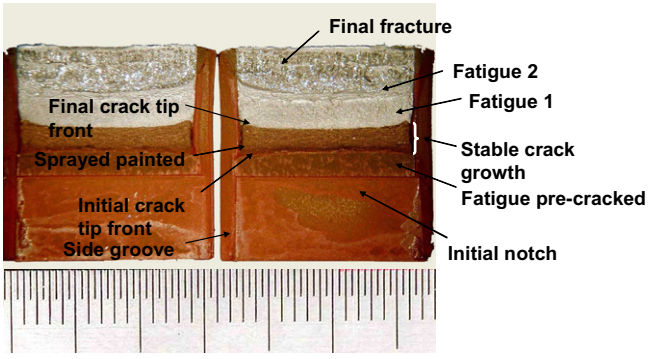

Fig. 4. Crack front visualization in a tested fracture toughness specimen.

This procedure leads to a more accurate definition of the *J*–*R* curve and to a lower dispersion of results. All the tests were ended at the catastrophic rupture of the specimen or after a stable ductile crack growth of 2 mm.

After correction, the resistance curves obtained for each configuration from the individual pairs (J, Δa) have been numerically fitted by means of expressions like:

$$J = C_1(\Delta a)^{C_2} \tag{8}$$

4. Results and discussion

Table 3 gives the yield strength of the two base metals and the weld metal measured at different temperatures and the corresponding mismatch ratios related. Although the metal yield strengths slightly increase as the temperature decreases, the temperature effect on the mismatch ratio is low and basically two mismatch ratios were obtained, giving way to an overmatching configuration with $M = 1.6$ and an undermatching configuration characterised by $M = 0.84$.

Fig. 5 shows the *J*–*R* curves obtained with the different tested configurations and temperatures in the case of the short ($a/W = 0.22$) and long cracks ($a/W = 0.5$). These figures also show the directly measured Δa values and the crack growth corresponding to cleavage (instability) fractures. In all the cases the temperature decrease does not modify the position of the *R*-curve but only the cleavage point, as the measured stable crack growth is larger as the temperature increases.

Fig. 6 now compares the results obtained with the different tested configurations. It is clearly seen that the specimen configuration modifies significantly the position of the *J*–*R* curve: the higher *J*-values for ductile propagation and also the steeper curves correspond to the overmatching configurations and specially to the case of a narrow weld, and among the undermatching configurations, it is the wide weld the one with the highest crack resistance to ductile crack growth, and the other short crack configuration give the same results as the long crack one. These results can be explained by the constraint effect. In this case the constraint is due to three different factors, the metal dissimilitude (material mismatch ratio, M), the crack length and the weld metal width.

Under a low constraint, as it is the case of the short crack overmatching welds ($M > 1$) and especially when the weld metal is narrow (configuration A), a higher J value need to be applied to make the crack to grow and, consequently, the fracture toughness will increase. Both, fracture initiation ($J_{0.2}$) and fracture propagation (*R*-curve gradient) significantly increase. In the case of undematching welds, due to a higher constraint, a severe reduction of fracture initiation and propagation was obtained. Finally, for the geometries with long cracks, characterised by a positive constraint parameter, the influence of varying both the mismatching ratio and the weld width is nearly non-significant.

Fig. 7 gives the ductile-to-brittle transition curves obtained with all these configurations when representing so the J values at cleavage (instability) or, in the ductile region, the J values after a crack growth of 2 mm. This figure clearly shows the important configuration effect on the transition temperature and also in the toughness values (J value) attained at any given temperature. Toughness is much higher at any temperature and the ductile-to-brittle temperature lower in the case of overmatching situations, when the crack has to grow in the weld metal confined by the presence of a metal base with a lower

Table 3
Base metal and weld metal yield strengths and mismatching coefficients.

T (°C)	σ_{0w} (MPa)	$\sigma_{0b(BM1)}$ (MPa)	$\sigma_{0b(BM2)}$ (MPa)	$M_{(BM1)}$	$M_{(BM2)}$
20	490	292	576	1.68	0.85
−20	499	308	586	1.62	0.85
−40	510	323	604	1.58	0.84
−60	514	335	619	1.54	0.83

Please cite this article in press as: Lezcano R et al. Effect of mechanical mismatching on the ductile-to-brittle transition curve of welded joints. Eng Fail Anal (2009), doi:10.1016/j.engfailanal.2009.04.030

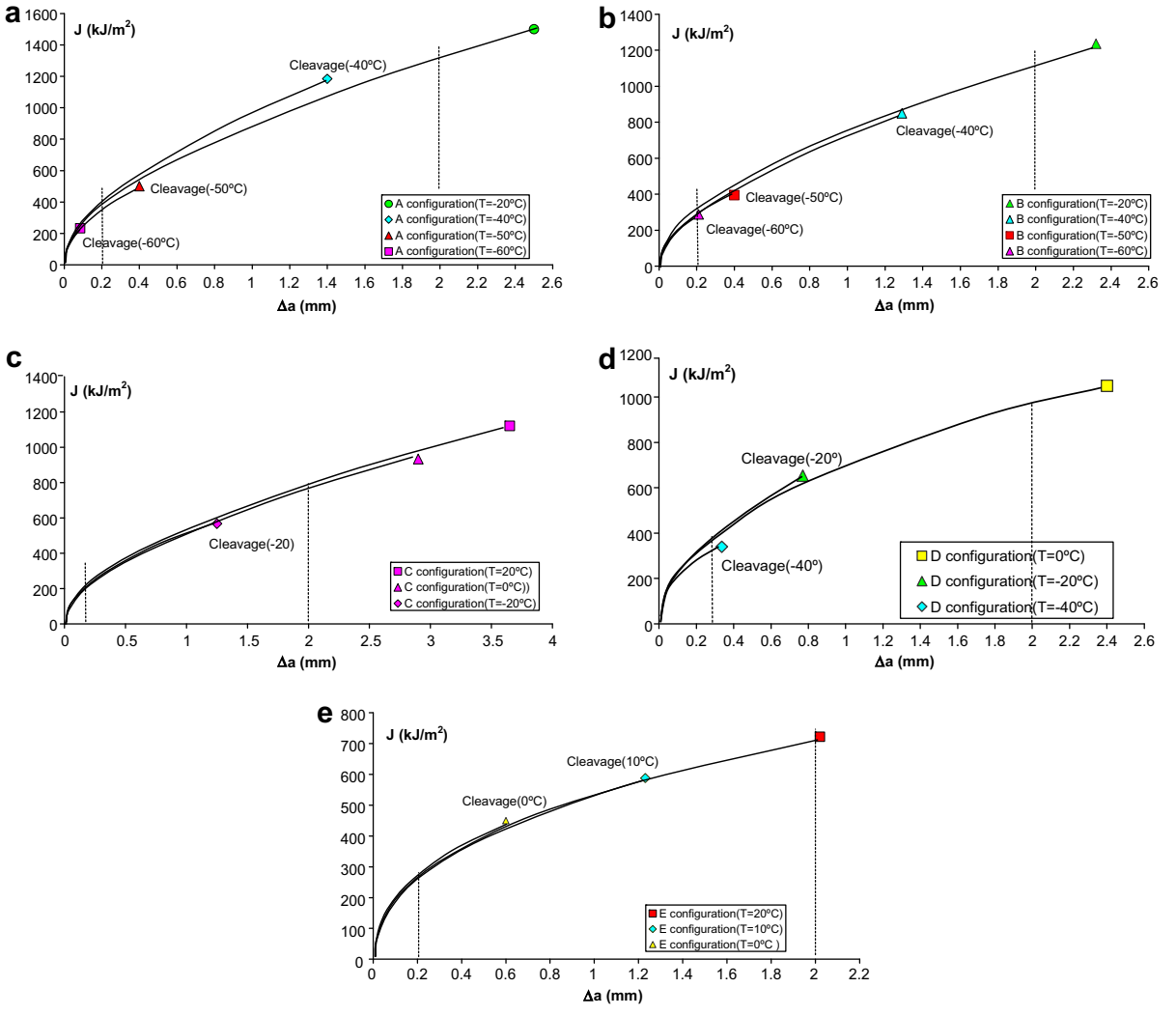

Fig. 5. *J–R* curve of the different configurations. (a) Overmatched, narrow weld, short crack, (b) overmatched, large weld, short crack, (c) undermatched, narrow weld, short crack, (d) undermatched, large weld, short crack, and (e) undermatched, large weld, long crack.

yield strength, and this fact is more relevant as the width of the weld zone is lower (configuration A). By the contrary, the high constriction developed when the crack is long enough (configuration E) gives way to a significant toughness decrease and also to the displacement of the transition curves to higher temperatures. A displacement of 50–60 °C was observed among the different studied configurations at an intermediate *J*-value of 550 kJ/m^2 calculated as the average between the ductile and brittle plateau values.

As a consequence of these results, over conservative assessments may arise from the application of high constraint toughness values to predict the behaviour of low constraint structural components. Ainsworth and O'Dowd [35] and the R6 defect assessment procedure [36] recommend to use two-parameter approaches within the context of a failure assessment diagram (FAD) methodology. The guidance within R6 defines the relationship between K_r and Q by means of the following expressions:

$$\begin{cases} K_r = \frac{K^C_{mat}}{K_{mat}} = 1, & Q \geqslant 0 \\ K_r = \frac{K^C_{mat}}{K_{mat}} = \left(1 + \xi \cdot (-Q)^k\right), & Q < 0 \end{cases} \tag{9}$$

where K_{mat} is the fracture toughness measured under high constraint, K^C_{mat} the fracture toughness corresponding to an specified level of constraint and ξ, k are parameters that define the toughness constraint sensitivity for the material and temperature of interest.

Please cite this article in press as: Lezcano R et al. Effect of mechanical mismatching on the ductile-to-brittle transition curve of welded joints. Eng Fail Anal (2009), doi:10.1016/j.engfailanal.2009.04.030

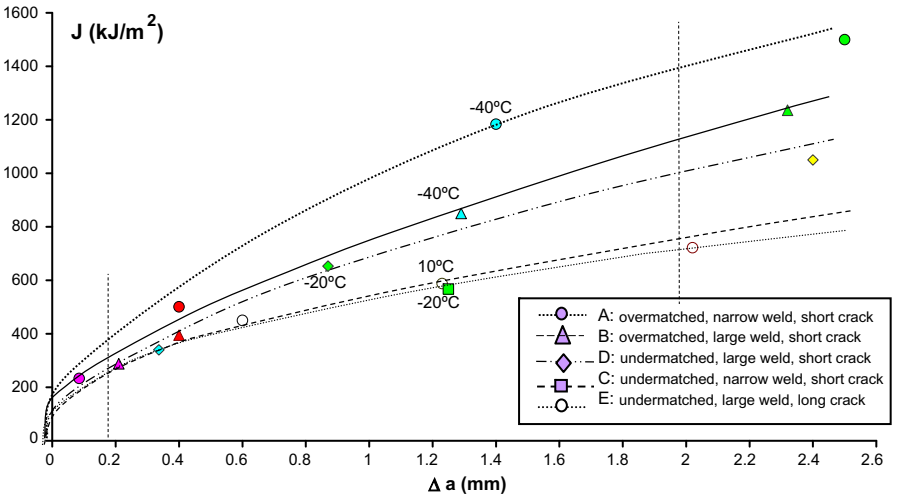

Fig. 6. Comparison of the *J*–*R* curves obtained with different configurations (−60 °C).

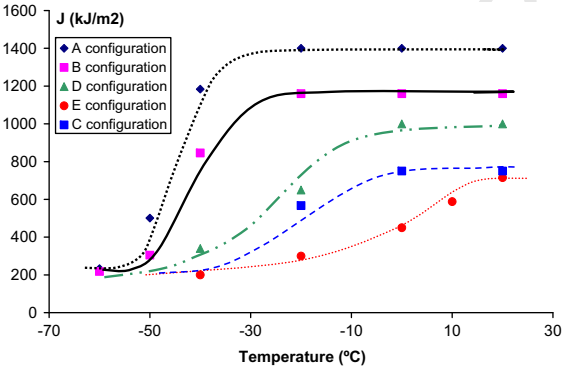

Fig. 7. Ductile-to-brittle transition curves of the different tested configurations.

In addition, the constraint modified fracture toughness can be expressed in terms of *J* as follows:

$$\begin{cases} J_r = \frac{J^C_{mat}}{J_{mat}} = 1, & Q \geqslant 0 \\ J_r = \frac{J^C_{mat}}{J_{mat}} = \left(1 + \xi \cdot (-Q)^k\right)^2, & Q < 0 \end{cases} \tag{10}$$

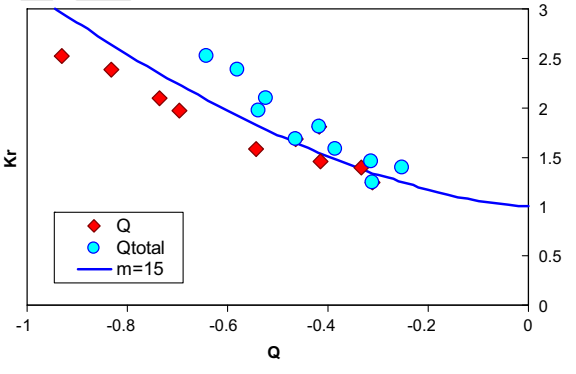

Fig. 8. Failure assessment diagram, in terms of the *Kr* fracture ratio against the total constraint *Q*-parameter.

Please cite this article in press as: Lezcano R et al. Effect of mechanical mismatching on the ductile-to-brittle transition curve of welded joints. Eng Fail Anal (2009), doi:10.1016/j.engfailanal.2009.04.030

where J_{mat} is the J value under high constraint and J^{C}_{mat} the J value at unstable fracture and specified level of constraint.

From Eqs. (9) and (10) is clear that $K_r = \sqrt{J_r}$.

Within these basis, Fig. 8 represents a failure assessment diagram, expressed in terms of the K_r fracture ratio against the total constraint Q-parameter (calculated in [7] for these configurations) using two different assumptions: first of all taking into account both, constraint due to geometry and constraint due to material mismatching (Q_{total}), and secondly taking into account constraint due only to geometry (that is, not taking into account the effect of material mismatching). In Fig. 8, K_r is derived from the experimental J-values obtained at catastrophic failure (cleavage fracture) divided by the T-stress value (T_c), Fig. 8 also shows the lower-bond curve for fracture that corresponds to the closed-form solution of Gao and Dodds [37] obtained using a shape parameter for the Beremin model ($m = 15$). This figure clearly shows that failure is predicted in a safe region if constraint due to material mismatching is not taken into account.

Although more experimental results would be needed to validate this particular aspect, the total constraint Q-parameter, which takes into account geometry and material mismatching, significantly modify the cleavage fracture behaviour. The lower the total constraint parameter is, the higher the J-value for cleavage fracture is; and this effect is especially important in the case of overmatching configurations with a narrow weld metal and short cracks.

5. Conclusions

An experimental program was conducted in order to assess the influence of material mismatching on the fracture toughness of welds, assuming a two material ideal weld. The level of material mismatching was defined by the mismatch ratio M, defined as the ratio between the weld metal and base metal yield strengths. Geometrical aspects, like the width of the weld zone and the length of the crack were also taken into account.

The fracture behaviour of the joints were determined at different temperatures using SE(B) specimens. The J-values for ductile crack growth were larger, the ductile-to-brittle transition curve was displaced towards lower-temperatures and higher-toughness values and the toughness for cleavage fracture was also larger in the case of overmatched joints, and all these effects were more significant as the weld width decreased. All these observations can be explained because of differences in constraint, as the fracture toughness increases when a loss of constraint occurs, as it is the case for overmatched joints, especially when the weld metal is narrow (material constraint) and when dealing with short cracks (geometrical constraint).

Acknowledgment

The authors acknowledge the financial support of FICYT (Regional R&D Program), Project IB05-157.

References

[1] Kirk MT, Dodds RH. The influence of weld strength mismatch on crack-tip constrain in single edge notch bend specimen. Int J Fract 1993;18:297–316.
[2] Toyoda M, Minami F, Ruggieri C, Thawlow C, Hauge M. Fracture property of HAZ-notched weld joint with mechanical mismatching – part I. Analysis of strength mismatching of welds on fracture initiation resistance of HAZ-notched joint. In: Shwalbe KH, Kocac MM, editors. Mismatching of welds, ESIS 17. London: Mechanical Engineering Publications; 1994. p. 399–415.
[3] Hao S, Schwalbe KH, Cornec A. The effect of yield strength mismatch on the fracture analysis of welded joints: slip-line field solutions for pure bending, I. J Solids Struct 2000;37:5385–411.
[4] Joch J, Ainsworth RA, Hyde TH. Limit load and J-estimates for idealised problems of deeply cracked welded joints in plane-strain bending. Fatigue and Fract Eng Mater Struct 1993;16:1061–79.
[5] Burstow MC, Ainsworth RA. Comparison of analytical, numerical and experimental solutions to problems of deeply cracked welded joints in bending. Fatigue Fract Eng Mater Struct 1995;18:221–34.
[6] Burstow M-C, Howard IC, Ainsworth RA. The influence of constraint on crack tip stress fields in strength mismatched welded joints. J Mech Phys Solids 1998;46:845–72.
[7] Betegón C, Peñuelas I. A constaint based parameter for quantifying the crack tip stress fields in welded joints. Eng Fract Mech 2006;73:1865–77.
[8] Kim YJ, Schwalbe KH. Numerical analysis of strength-mismatch effect on local stresses for ideally plastic materials. Eng Fract Mech 2004;71:1177–99.
[9] Betegón C, Hancock JW. Two-parameter characterization of elastic–plastic crack-tip fields. J Appl Mech 1991;58:104–10.
[10] Du ZZ, Hancock JW. The effect of non-singular stresses on crack tip constraint. J Mech Phys Solids 1991;39:555–67.
[11] O'Dowd NP, Shih CF. Family of crack-tip fields characterization by a triaxiality parameter – I. Structure of fields. J Mech Phys Solids 1991;39:989–1015.
[12] O'Dowd NP, Shih CF. Family of crack-tip fields characterization by a triaxiality parameter – II. Fracture application. J Mech Phys Solids 1992;40:939–63.
[13] Hutchinson JW. Singular behaviour at the end of a tensile crack in a hardening material. J Mech Phys Solids 1968;16:13–31.
[14] Rice JR, Rosengren GF. Plane strain deformation near a crack tip in a power-law hardening material. J Mech Phys Solids 1968;16:1–12.
[15] Zhang ZL, Hauge M, Thaulow C. Two parameter characterisation of the near tip stress field for a bi-material elastic–plastic interface crack. Int J Fract 1996;79:65–83.
[16] Zhang ZL, Thaulow C, Hauge M. Effects of crack size and weld metal mismatch on the HAZ cleavage fracture toughness of wide plates. Eng Fract Mech 1997;57:653–64.
[17] Amar E, Pineau A. Application of a local approach to ductile–brittle transition in a low-alloyed steel. Nucl Eng Des 1987;105:89–96.
[18] Gao X, Shih CF, Tvergaard V, Needlman A. Constraint effects on the ductile–brittle transition in small scale yielding. J Mech Phys Solids 1996;44(8):1255–82.
[19] Hausild P, Berdin C, Bompard P. Prediction of cleavage fracture for a low-alloy steel in the ductile-to-brittle transition temperature range. Mater Sci Eng A 2005;391:188–97.
[20] Betegón C, Peñuelas I, del Coz JJ. Numerical análisis of material mismatching in the transition curve of welded joints. Eng Fract Mech 2008;75(11):3464–82.
[21] Beremin FM. A local criterion for cleavage fracture of a nuclear pressure vessel steel. Metal Mater Trans A 1983;14(A):2277–87.

Please cite this article in press as: Lezcano R et al. Effect of mechanical mismatching on the ductile-to-brittle transition curve of welded joints. Eng Fail Anal (2009), doi:10.1016/j.engfailanal.2009.04.030

[22] Wasiluk B, Petti JP, Dodds RH. Temperature dependence of Weibull stress parameters: Studies using the Euro-material. Eng Fract Mech 2006;73:1046–69.
[23] Zang ZL, Thaulow C, Odegard J. A complete Gurson model approach for ductile fracture. Eng Fract Mech 2000;67:155–68.
[24] Gurson AL. Continuum theory of ductile rupture by void nucleation and growth: part I – yield criteria and flow rules for porous ductile media. J Eng Mater Technol 1977;99:2–15.
[25] Tvergaard V. Influence of voids on shear bands instabilities under plane strain conditions. Int J Fract 1981;17:389–407.
[26] Tvergaard V. On localization in ductile materials containing spherical voids. Int J Fract 1982;18:157–69.
[27] Tvergaard V. Material failure by void growth to coalescence. Adv Appl Mech 1990;27:83–151.
[28] Tvergaard V, Needleman A. Analysis of cup-cone fracture in a round tensile bar. Acta Metall 1984;32:57–169.
[29] Thomason PF. Ductile fracture of metals. Oxford: Pergamon Press; 1990.
[30] Thomason PF. A view of ductile-fracture modelling. Fatigue Fract Eng Mater Struct 1998;21:1105–22.
[31] Pardoen T, Hutchinson JW. An extended model for void growth and coalescence. J Mech Phys Solids 2000;48:2467–512.
[32] ASTM E8M-04. Standard test method of tension testing of metallic materials [Metrics]. Annual book of ASTM standards, vol. 03-01; 2006.
[33] Peñuelas I, Betegón C, Rodríguez C. A failure model applied to the determination of the fracture toughness of welded joints. Numerical simulation and experimental validation. Eng Fract Mech 2006;73:2756–73.
[34] ASTM E1820-05a. Standard test method for measurement of fracture toughness. Annual book of ASTM standards, vol. 03-01; 2006.
[35] Ainsworth RA, O'Dowd NP. Constraint in the failure assessment diagram approach for fracture assessment. ASME. J Press Ves Technol 1995;117:60–267.
[36] R6: Assessment of the integrity of structures containing defects. British Energy Generation Limited; 2001 [revision 4].
[37] Gao X, Dodds RH. An engineering approach to assess constraint effects on cleavage fracture toughness. Eng Fract Mech 2001;68:263–83.

Please cite this article in press as: Lezcano R et al. Effect of mechanical mismatching on the ductile-to-brittle transition curve of welded joints. Eng Fail Anal (2009), doi:10.1016/j.engfailanal.2009.04.030